

Non-viral systemic delivery of siRNA or antisense oligonucleotides targeted to Jun N-terminal kinase 1 prevents cellular hypoxic damage

Seema Betigeri · Min Zhang · Olga Garbuzenko · Tamara Minko

Published online: 14 December 2010

© The Author(s) 2010. This article is published with open access at Springerlink.com

Abstract Many pathological conditions and environmental impacts lead to the development of severe tissue hypoxia that aggravates the primary disorder, provokes cell death, and limits the patient's recovery. We hypothesized that suppression of Jun N-terminal kinase 1 (JNK1) will limit tissue damage induced by severe hypoxia. To test the hypothesis, antisense oligonucleotides (ASO) or small interfering RNA (siRNA) targeted to JNK1 mRNA were incorporated or complexed with neutral or cationic liposomes, respectively, and administered systemically to mice prior to hypoxia exposure. The animals were placed in a special chamber ventilated with room air (normoxia) or a gas mixture containing 6% O₂ and 94% N₂ (hypoxia). Liposomes, ASO, and siRNA were found to accumulate in the lungs, kidney, spleen, and heart. Only trace amounts of liposomes and their payloads (ASO and siRNA) were found in the brain. The down regulation of JNK1 protein limited activation of cell death signal, apoptotic, and necrotic tissue damage under hypoxic conditions. Consequently, we were able to verify our hypothesis and provide proof of concept of a unique approach to the prevention of cellular hypoxic damage by the suppression of JNK1 signaling pathways after the efficient delivery of ASO or siRNA.

Keywords Liposomal delivery of nucleic acids · Hypoxia · Apoptosis and necrosis · Body distribution of siRNA and antisense oligonucleotides

Introduction

Many environmental factors as well as endogenous disturbances in blood oxygenation and circulation are often associated with limitations in the oxygen delivery to tissues and cells. Severe deprivation in adequate oxygen supply may cause marked tissue damage and finally lead to hypoxic cell death (Busl and Greer 2010; Goni-de-Cerio et al. 2007; Hossain 2008; Minko et al. 2002; Minko et al. 2005; Soleymanlou et al. 2007; Vacotto et al. 2008). Moreover, reoxygenation—a restoration of oxygen supply to the formerly hypoxic tissues as a result of the treatment, compensatory reactions of an organism, or ending of exogenous hypoxic conditions may lead even to more pronounced tissue damage (Dhar-Mascareno et al. 2005; Freiberg et al. 2006; Hung and Burton 2006; Kim et al. 2007; Ricci et al. 2009; Yajima et al. 2009). Despite substantial differences in the physiological conditions during hypoxia and reoxygenation, the main mechanisms of tissue damage under both settings are quite similar. The major mechanisms include disturbances in cellular metabolism, mitochondrial dysfunctions, disturbances in acid–base homeostasis, oxidative stress damage by active oxygen and nitrogen species, and apoptotic and necrotic cell death (Blokina and Fagerstedt 2010; Boning et al. 2008; Cho et al. 2007b; Gonchar and Mankovskaya 2009; Kim et al. 2004; Kim and Park 2003; Kothari et al. 2003; Minko et al. 2002; Minko et al. 2005; Murray et al. 2003; Portugal-Cohen and Kohen 2009; Surova et al. 2009; Vacotto et al. 2008; Yajima et al. 2009). Consequently, the suppression of the above-mentioned mechanisms of hypoxic cellular damage can potentially be used in effective therapy of many diseases associated with hypoxia and/or reoxygenation and to increase the resistance to damaging environmental factors. Several approaches have been recently proposed including preliminary adaptation to

S. Betigeri · M. Zhang · O. Garbuzenko · T. Minko (✉)
Department of Pharmaceutics, Ernest Mario School of Pharmacy,
Rutgers, The State University of New Jersey,
160 Frelinghuysen Road,
Piscataway, NJ 08854-8020, USA
e-mail: minko@rci.rutgers.edu

hypoxia, stress, and other environmental factors (Boning et al. 2008; Corbucci et al. 2005; Gonchar and Mankovskaya 2009; Meerson et al. 1994; Millet et al. 2010; Ostadal and Kolar 2007; Zhao et al. 2009) as well as many pharmacological methods (Betigeri et al. 2006; Carlsson et al. 2009; Cho et al. 2007a; Danielyan et al. 2006; Lecour et al. 2006; Minciu Macrea et al. 2010; Minko et al. 2002; Minko et al. 2005; Myllyharju 2008; Nagel et al. 2010; Surova et al. 2009; Wenger et al. 2009; Zhu et al. 2008).

Hypoxia inducible factor one alpha (HIF1A) protein is a key initiator of cell death signal under hypoxic conditions (Hellwig-Burgel et al. 2005). We investigated the role of this protein as a possible target for the remediation of hypoxic cellular damage and found that HIF1A plays a bimodal role during hypoxia (Wang and Minko 2004; Wang et al. 2004; Wang et al. 2008). On the one hand, activation of HIF1A during hypoxia initiates cell death signal inducing apoptosis (programmed cell death or cellular suicide) and necrosis (pathological cell death). On the other hand, overexpression of HIF1A boosts the power of anti-hypoxic systems that increase cellular resistance to hypoxia.

Recently, we identified Jun N-terminal kinase 1 (JNK1), another major player in the activation of apoptosis signaling pathways and hypoxic damage from the mitogen-activated protein kinases (MAPK) family of proteins, as a prospective target for pharmacological prevention of cellular damage during severe hypoxia (Betigeri et al. 2006). It has been shown that JNK1 as a stress-activated protein kinase can be induced by inflammatory cytokines, bacterial endotoxin, osmotic shock, UV radiation, and hypoxia (Bennett et al. 2001; Chihab et al. 1998; Zhou et al. 2004). Analysis of literature data (Bennett et al. 2001; Derijard et al. 1994; Karin 1995) showed that cellular hypoxic damage can be induced by the pathway presented in Fig. 1. Induction of JNK by hypoxia mediates phosphorylation of activating transcriptional factor-2 (ATF2) and c-Jun and stimulates their transcriptional activities leading to *c-Jun* activation. The newly synthesized c-Jun protein combines with c-Fos protein to form stable transcriptional factor activator protein-1 (AP1) heterodimers. The formation of AP1 is a key step following the induction of central cell death signal leading to the activation of caspase-dependent apoptosis signal pathways and finally causing cell death. It was found that c-Jun N-terminal kinase 1 (JNK1, SAPK1 and MAPK8) plays a central role in the development of cellular damage under hypoxia, hypoxia/reoxygenation, and ischemia/reperfusion conditions (Crenesse et al. 2003; Garay et al. 2000; Hreniuk et al. 2001). The *in vitro* data previously obtained in our laboratory showed that the suppression of JNK1 by antisense oligonucleotides (ASO) or small interfering RNA (siRNA) targeted to JNK1 mRNA substantially limited cellular mortality after severe hypoxia (Betigeri et al. 2006). The present study is a logical

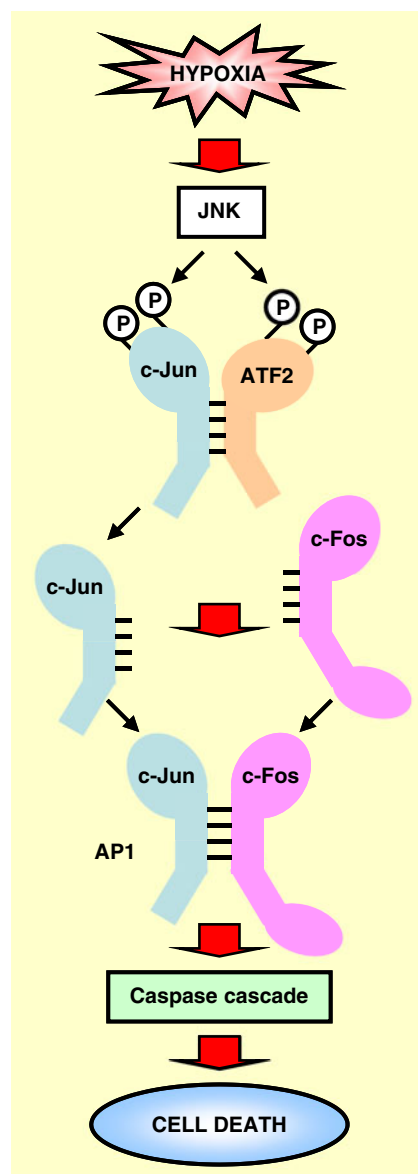


Fig. 1 Schema of apoptosis induction by hypoxia. Activation of Jun N-terminal kinase (*JNK*) by hypoxia mediates phosphorylation of activating transcriptional factor-2 (*ATF2*) and c-Jun and stimulates their transcriptional activities. The newly synthesized c-Jun protein combines with c-Fos protein to form stable transcriptional factor activator protein-1 (*AP1*) heterodimers. The formation of AP1 activates caspase-dependent apoptosis signal and finally induces cell death

continuation of our previous work and is aimed at *in vivo* testing of this approach.

Material and methods

Liposomal compositions of siRNA and ASO

Negatively charged siRNA was delivered by cationic liposomes (N-[1-(2,3-Dioleoyloxy) propyl]-N,N,N-trimethylam-

monium methylsulfate, DOTAP, Avanti Polar Lipids, Alabaster, AL). ASO targeted to JNK1 mRNA (5'-CTC TCT GTA GGC CCG CTT GG-3') (Garay et al. 2000) and ASO labeled with fluorescein isothiocyanate (FITC) were synthesized by Oligos Etc. (Wilsonville, OR). The DNA backbone of all bases in oligonucleotides was P-ethoxy modified in order to eliminate electrical charge and increase incorporation efficacy into "neutral" PEGylated liposomes. Liposomes were prepared as described previously (Garbuzenko et al. 2009; Garbuzenko et al. 2010; Pakunlu et al. 2006). Briefly, to prepare PEGylated liposomes, egg phosphatidyl choline, cholesterol, and DSPE-PEG (1,2-distearoyl-sn-glycero-3-phosphoethanolamine-*N*-aminopolyethylene glycol- $M_w \sim 2,000$ ammonium salt) were dissolved in 4.0 ml of chloroform at 1.85:1:0.15 molar ratio, respectively (all compounds were obtained from Avanti Polar Lipids, Alabaster, AL). The clear lipid solution was evaporated at 25°C under reduced pressure. A thin layer was formed and rehydrated using 2.0 ml of 0.3 M sodium citrate buffer (pH=4.0). ASO was loaded into liposomes by dissolving in rehydration buffer at concentration 0.5 mM. The lipid mixture was sonicated continuously for 3.0 h to obtain stealth liposomes. Liposomes were extruded gradually through 100 and 200 nm polycarbonate membranes at room temperature using an extruder device from Northern Lipids, Inc. (Vancouver, BC, Canada). Liposomes were separated from non-encapsulated ASO by dialysis against 100 volumes of 0.9% NaCl. The encapsulation efficacy of ASO was ~50–60%, respectively. The final phospholipids concentration was 10 mg/ml. Mean diameter of "neutral" liposomes was 100–140 nm. siRNA targeted to exon 1 JNK1 mRNA (sense sequence—3'-GGA GCU CAA GGA AUA GUA UTT-5') was selected based on the results of our previous studies (Betigeri et al. 2006) and synthesized according to our design by Ambion (Austin, TX). A siGLO Green 6-FAM transfection indicator was purchased from Dharmacon, Inc. (Chicago, IL). siRNA possess negative charges requiring positively charged (cationic) liposomes to form stable complexes. Cationic liposomes were prepared from positively charged DOTAP at concentration 5 mg/mL using thin layer procedure as previously described (Betigeri et al. 2006; Garbuzenko et al. 2009), followed by extrusion through 100 nm polycarbonate membrane. The siRNA was dissolved in RNase free water at a concentration of 400 μ M. To this solution, appropriate volume of DOTAP (5 mg/mL) was added, mixed by pipette and incubated for 30 min at room temperature. The molar ratio of siRNA/DOTAP was ~1:100. Resulting siRNA-cationic liposome complex was used in the studies. siGLO Green was dissolved in RNase free solution to the final concentration of 200 μ M. DOTAP liposomes were mixed with siGLO in the ration 6:1 v/v and incubated at room temperature for 15 min before use. Mean DOTAP/siGLO complex size was around 500 nm. Aliquots

of each liposomal formulation were labeled with near infrared fluorescent dye Cy5.5 Mono NHS Ester (GE Healthcare, Amersham, UK). A fluorescent dye was dissolved together with lipids in chloroform. Approximate excitation/emission maxima of all fluorescent substances used in the study are: 675/694 nm (Cy5.5); 520/594 nm (siGLO Green, siRNA labeled with 6-FAM dye); 494/518 nm (FITC).

Liposome size and zeta potential

Particle size was measured by dynamic light scattering using 90 Plus Particle Sizer Analyzer (Brookhaven Instruments Corp., New York, NY). Aliquot of 40 μ L of each sample was diluted in 2 mL of saline. Zeta potential was measured on PALS Zeta Potential Analyzer (Brookhaven Instruments Corp, New York, NY). Samples were taken as is and their volume was 1.5 mL. All measurements were carried out at room temperature. Each parameter was measured in triplicate, and average values were calculated.

Cell line

The human embryonic kidney 293 cells were obtained from American Type of Tissue Culture (Manassas, VA). Cells were cultured in Dulbecco's modified Eagle's medium (GIBCO Inc., Cincinnati, OH) supplemented with 10% fetal bovine serum (Fisher Chemicals, Fairlawn, NJ). All experiments were performed on cells in the exponential growth phase.

Cellular uptake and localization of liposomes, ASO and siRNA

Cellular internalization of liposomes, ASO and siRNA were monitored by fluorescence microscopy. Four series of the experiments were carried out: (1) "neutral" liposomes labeled with Cy5.5 (red fluorescence); (2) cationic liposomes labeled with Cy5.5 (red fluorescence); (3) ASO labeled with FITC (green fluorescence) delivered by "neutral" liposomes; and (4) siRNA labeled with 6-FAM (siGLO Green, green fluorescence) delivered by cationic liposomes. Cells were separately incubated for 24 h at 37°C with each liposomal formulation.

Animal model of hypoxia exposure

Experiments were performed on healthy 6–8 weeks old SKH1-hr hairless mice (25–35 g) obtained from Charles River Laboratories (Wilmington, MA). Veterinary care followed the guidelines described in the guide for the care and use of laboratory animals as well as the requirements established by the animal protocol approved by the Rutgers Institutional Animal Care and Use Committee. All mice were contained in micro-isolated cages under pathogen free

conditions at room temperature with humidity of $40 \pm 15\%$ and light/dark cycle on 12 h per day in the animal maintenance facility. Normobaric hypoxia was created in a $300 \times 350 \times 600$ mm Plexiglas chamber specifically designed for this project by Billups-Rothenberg, Inc. (Del Mar, CA). Hypoxia was induced by subjecting the chamber to a constant flow (15–20 l/min) of hypoxic gas mixture containing 6% oxygen and 94% nitrogen. The oxygen concentration in the chamber was continuously monitored using an oxygen analyzer (Vascular Technology, Inc., Nashua, NH). A heating pad was placed inside the Plexiglass chamber to maintain the body temperature of the mice. All animals were placed in the chamber for 2 h. Prior to exposure, mice were pretreated with 100 μ L of different formulations by intravenous injection. Mice were randomized into six experimental groups: (1) normoxia (room air, 21% O₂) following injection of saline; (2) hypoxia (6% O₂) following injection of saline; (3) hypoxia (6% O₂) following injection of neutral liposomes; (4) hypoxia (6% O₂) following injection of cationic liposomes; (5) hypoxia (6% O₂) following injection of neutral liposomes with ASO targeted to JNK1 mRNA; (6) hypoxia (6% O₂) following injection of cationic liposomes with siRNA targeted to JNK1 mRNA. The doses of ASO and siRNA were 13 nmoles per mouse (80 and 173 μ g ASO and siRNA, respectively). After the treatment, all mice were anesthetized with isoflurane and euthanized. The organs (lungs, heart, liver, kidney, spleen, and brain) were excised and used for the evaluation of body distribution of liposomes and their payloads (siRNA and ASO), study of lactic acid, apoptosis, gene and protein expression and histopathological analysis.

Content of liposomes in different organs

The distribution of fluorescent-labeled “neutral” and cationic liposomes and their payloads (ASO and siRNA) was examined in mouse lungs, heart, liver, spleen, and kidneys. The organs were excised, rinsed in saline, and fluorescence was registered by IVIS imaging system (Xenogen Corporation, Alameda, CA). Visible light and fluorescence images were taken and overlaid. The intensity of fluorescence was represented on composite light/fluorescent images by different colors with blue color reflecting the lowest fluorescence intensity and red color—the highest intensity. Images of each organ were then scanned and total fluorescence intensity was calculated by a special computer program originally developed for our laboratory by Dr. V. P. Pozharov as previously described (Garbuzenko et al. 2009; Garbuzenko et al. 2010). Preliminary experiments showed a strong linear correlation between the total amount of labeled substance accumulated in the organ and calculated total fluorescence intensity. The fluorescence was expressed in arbitrary units with 1 unit represented approximately 2×10^{10} photons/s/sr/cm². The

method allows a quantitative comparison of the concentration of the same fluorescent dye between different series of the experiments. The mass of all organs was measured. No statistical differences were found in the mass of the same organ between all experimental groups of animals. The fluorescence intensity was normalized for organ weight.

Lactic acid and protein concentration

Approximately 30–40 mg of tissues was weighed, lysed in Ripa buffer (Santa Cruz Biotechnologies, Inc., Santa Cruz, CA) and homogenized using Ultra Turrax T-25 basic homogenizer (IKA Works, Wilmington, NC). To confirm the existence of cellular hypoxia, the concentration of lactic acid in tissue homogenates was measured by an enzymatic assay kit (Sigma, St. Louis, MO) and was expressed per g of protein determined using the BCA protein assay kit (Pierce, Rockford, IL).

Gene expression

Quantitative reverse transcriptase-polymerase chain reaction (RT-PCR) was used for the analysis of genes encoding JNK1, caspase 9, and β -actin as previously described (Betigeri et al. 2006; Dharap et al. 2005; Minko et al. 1999; Pakunlu et al. 2003; Pakunlu et al. 2004; Wang et al. 2004). RNA was isolated using an RNeasy kit (Qiagen, Valencia, CA). The following pair of primers were used: JNK1, 5'-TTGGAACACCATGTCCTGAA-3' (sense) and 5'-ATG TAC GGG TGT TGG AGA GC-3' (antisense); caspase 9, 5'-TGA CTG CCA AGA AAA TGG TG-3' (sense) and 5'-CAG CTG GTC CCA TTG AAG AT-3' (antisense); and β -actin, 5'-GAC AAC GGC TCC GGC ATG TGC A 3' (sense) and 5'-TGA GGA TGC CTC TCT TGC TCT G-3' (antisense). Gene expression was calculated as the ratio of analyzed RT-PCR product to the internal standard (β -actin).

Protein expression

To confirm RT-PCR data the expression of JNK1 protein and caspase 9 were measured by two methods: Western immunoblotting analysis and immunohistochemistry. The identification of the above proteins was conducted by Western immunoblotting analysis and processed using scanning densitometry to quantify the expressed proteins. To this end, approximately 30–40 mg of the tissue from each organ was weighed, lysed in Ripa buffer (Santa Cruz Biotechnologies, Inc., Santa Cruz, CA), and homogenized using Ultra Turrax T-25 basic homogenizer (IKA Works, Wilmington, NC). Following incubation on ice for 45 min, the tissues were centrifuged at $10,000 \times g$ for 10 min. Protein content in the supernatant was determined using the BCA Protein Assay Kit (Pierce, Rockford, IL) and 40 μ g of

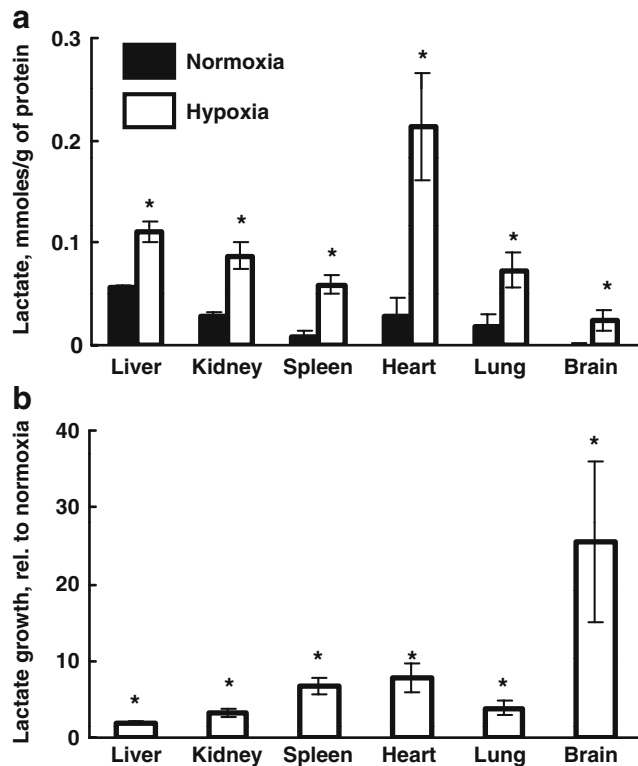


Fig. 2 Accumulation of lactic acid in different organs under hypoxia. **a** Absolute values. **b** Lactic acid growth under hypoxia relative to normoxia values. Hypoxia was induced in mice by the inhalation of gas mixture containing 6% O₂ for 2 h. Means±SD are shown. **P*< 0.05 when compared with normoxia

protein was run on a 15% sodium dodecyl sulphate (SDS) polyacrylamide gel immersed in Tris/Glycine/SDS buffer (BioRad, Hercules, CA) for 90 min at 70 V. Proteins were transferred to an Immobilon-P nitrocellulose membrane (Millipore, Bedford, MA) in a Tris/Glycine buffer (BioRad, Hercules, CA) for 90 min at 100 V. The membrane was blocked in non-fat milk for 2 h at room temperature on a rotating shaker to prevent non-specific binding, washed and incubated overnight with anti-JNK1 mouse primary antibody (1:2,000 dilution, Cell Signaling Technology, Inc., Beverly, MA), anti-caspase 9 rabbit primary antibody (1:2,000 dilution, Stress Gen Biotechnologies, Victoria State, BC Canada) and anti- β -actin mice primary antibody (1:2,000 dilution, Oncogene Research, San Diego, CA) at 4°C. Following further washing, the membrane was immersed in goat anti-rabbit and goat anti-mouse IgG biotinylated antibodies (1:3,000 and 1:1,000 dilution, respectively, BioRad, Hercules, CA) at room temperature for 1.5 h on a rotating shaker. Bands were visualized using an alkaline phosphatase color development reagent (BioRad, Hercules, CA). The bands were digitally photographed and scanned using Gel Documentation System 920 (NucleoTech, San Mateo, CA). β -actin was used as an internal standard to normalize protein expression. Protein expression was calculated as the ratio of

mean band density of the analyzed protein to that of the internal standard (β -actin). The identification of the JNK1 protein was also made by immunohistochemical staining of paraffin embedded tissue sections. After deparaffinization and rehydration, the slides were stained using Vector® M.O.M. Immunodetection Kit (Vector Laboratories, Inc., Burlingame, CA). Mouse monoclonal antibody to JNK1 (Cell Signaling Technology, Inc., Beverly, MA, 1:40 dilution) was used as the primary antibody for detection. Biotinylated anti-mouse IgG Reagent (1:250 dilution, Vector Laboratories, Inc., Burlingame, CA) and HSP-Streptavidine Detection System (1:500 dilution, Vector Laboratories, Inc., Burlingame, CA) in combination with DAB substrate kit for peroxidase were used for visualization. After staining, the slides were analyzed by light microscopy and photographed.

Apoptosis

Apoptosis was analyzed by measuring the enrichment of histone-associated DNA fragments (mono- and oligonucleosomes) in the cell cytoplasm using anti-histone and anti-DNA antibodies by a cell death detection ELISA Plus kit (Roche, Nutley, NJ) as previously described (Dharap et al. 2005; Pakunlu et al. 2004; Wang et al. 2004).

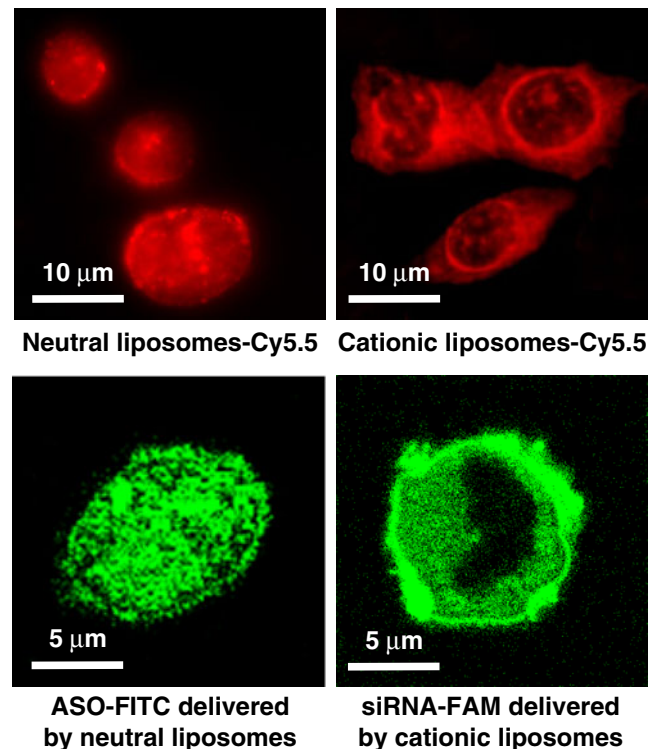


Fig. 3 Intracellular localization of neutral and cationic liposomes, antisense oligonucleotides (ASO) and siRNA delivered by neutral and cationic liposomes, respectively. Representative fluorescence images of cells incubated 120 min with substances indicated. Neutral and cationic liposomes were labeled by Cy5.5 (red), ASO were labeled by FITC (green), siRNA were labeled by FAM (siGLO Green)

Histopathological examination

After sacrificing animals, the organs were excised and immediately fixed in 10% phosphate-buffered formalin. Samples were subsequently dehydrated and embedded in Paraplast®. Five-micrometer slides were cut and stained with hematoxylin-eosin and analyzed.

Statistical analysis

Data obtained were analyzed using descriptive statistics, single-factor analysis of variance, and presented as mean values±the standard deviation (SD) from four to eight independent measurements in separate experiments. The comparison among groups was performed by the independent sample Student's *t* tests. The difference between variants is considered significant if $P < 0.05$.

Results

Particle size and zeta potential

Our data showed that the size of all formulations of “neutral” liposomes (empty and with ASO) was 100–140 nm. The average size of empty cationic liposomes and DOTAP/siRNA complexes was 120 and 500 nm, respectively. “Neutral” liposomes had a slight negative charge (-10 ± 2 mV). DOTAP liposomes had a positive charge ($+25 \pm 4$ mV). The formation of DOTAP/siRNA complexes decreased the surface charge to $+4 \pm 2$ mV likely due to the electrostatic interactions between positively charged lipid and negatively charged siRNA.

Development of tissue hypoxia

The accumulation of lactic acid in tissues was used as a hallmark of the development of severe tissue hypoxia in different organs of mice during exogenous hypoxia. Data obtained show that the exposure of mice to 6% O₂ in the inspired gas mixture led to a significant increase of the absolute concentration of lactic acid in all studied organs within 2 h (Fig. 2a). The most dramatic relative increase in the lactic acid concentration in tissues was registered in the brain, heart, spleen, and lungs (Fig. 2b). These data clearly show that the experimental conditions used led to the development of a severe tissue hypoxia in many organs of mice exposed to the hypoxic gas mixture.

Delivery of ASO and siRNA

Our previous findings showed that naked ASO and siRNA poorly penetrate cellular plasma membrane and therefore

require special delivery systems for efficient intracellular uptake (Patil et al. 2008; Wang et al. 2008). Consequently, neutral and cationic phospholipid liposomes were used to deliver neutral P-ethoxy ASO and negatively charged siRNA, respectively. In vitro data obtained in the present study demonstrate that liposomes provide for an effective intracellular delivery of both ASO and siRNA (Fig. 3). Delivered by liposomes ASO were distributed homogenously in the cytoplasm and nucleus of exposed cells, while siRNA was accumulated predominately in the cytoplasm. These data allowed us to use both types of liposomes for systemic delivery of ASO and siRNA in vivo. The analysis of body distribution of liposomes and delivered payload showed that the content of liposomes, ASO and siRNA per gram of wet tissue was highest in the lungs. In contrast, only trace amounts of liposomes and payload were found in the brain. A substantial amount of ASO or siRNA was found in the heart (Fig. 4). Based on the organ content of active components as well as on the degree of tissue hypoxia, we selected the lungs (the highest ASO or siRNA accumulation and moderate

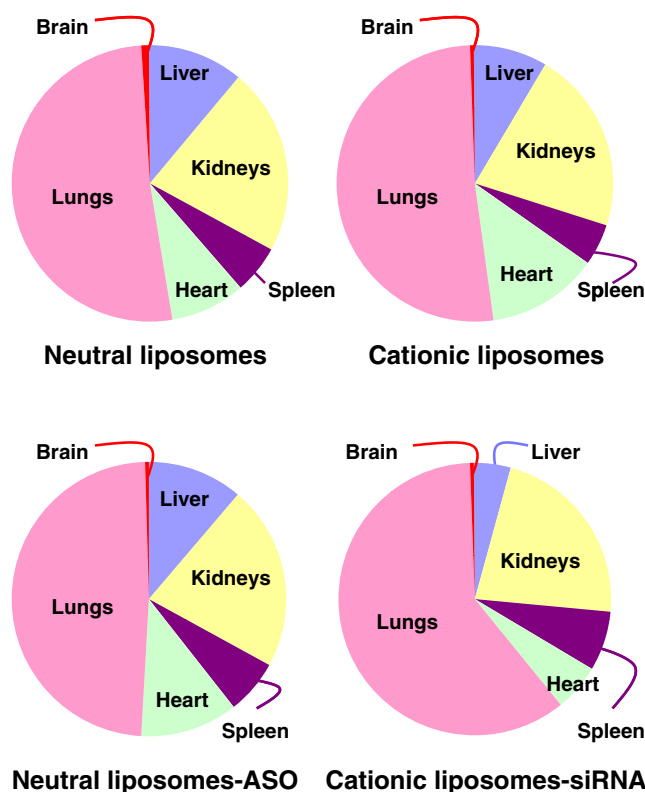


Fig. 4 Relative tissue content of empty neutral and cationic liposomes, antisense oligonucleotides (ASO) and small interfering RNA (siRNA) in different organs. Neutral P-ethoxy ASO and negatively charged siRNA were delivered by neutral and cationic liposomes, respectively. Liposomes, ASO and siRNA were labeled with fluorescent dyes and intravenously injected to hairless mice. Two hours after treatment mice were euthanized, organs were excised, fluorescence was registered by IVIS imaging system and normalized per gram of tissue weight in each organ

hypoxia), heart (moderate hypoxia and moderate ASO or siRNA accumulation) and brain (the highest hypoxia and the lowest ASO or siRNA accumulation) for further detailed study.

Suppression of JNK1 protein

Suppression of the targeted JNK1 mRNA and protein by ASO or siRNA delivered by liposomes was studied by RT-PCR and immunohistochemical protein staining. The results showed that hypoxia led to the significant overexpression of the JNK1 gene and protein (Fig. 5a (bar 2), b for the gene and protein, respectively). Empty neutral or cationic liposomes did not have a significant influence on this overexpression (Fig. 5a (bars 3 and 4), b). Treatment of mice with liposomes containing ASO or siRNA targeted to

JNK1 mRNA led to a substantial decrease in the expression of this gene and protein in the lungs and heart under hypoxic conditions (Fig. 5a (bars 5 and 6), b). In contrast, treatment of mice with liposomes contained JNK1 ASO or siRNA did not influence the expression of either the mRNA or protein in the brain under hypoxic exposure. In general, one can conclude that the efficiency of the suppression of targeted JNK1 mRNA and protein correlated with the organ content of delivered ASO or siRNA.

Inhibition of hypoxic cell damage and death

To examine the hypoxic cellular damage and influence of the suppression of JNK1 on this process, we carried out a histopathological analysis (hematoxylin-eosin stain) and

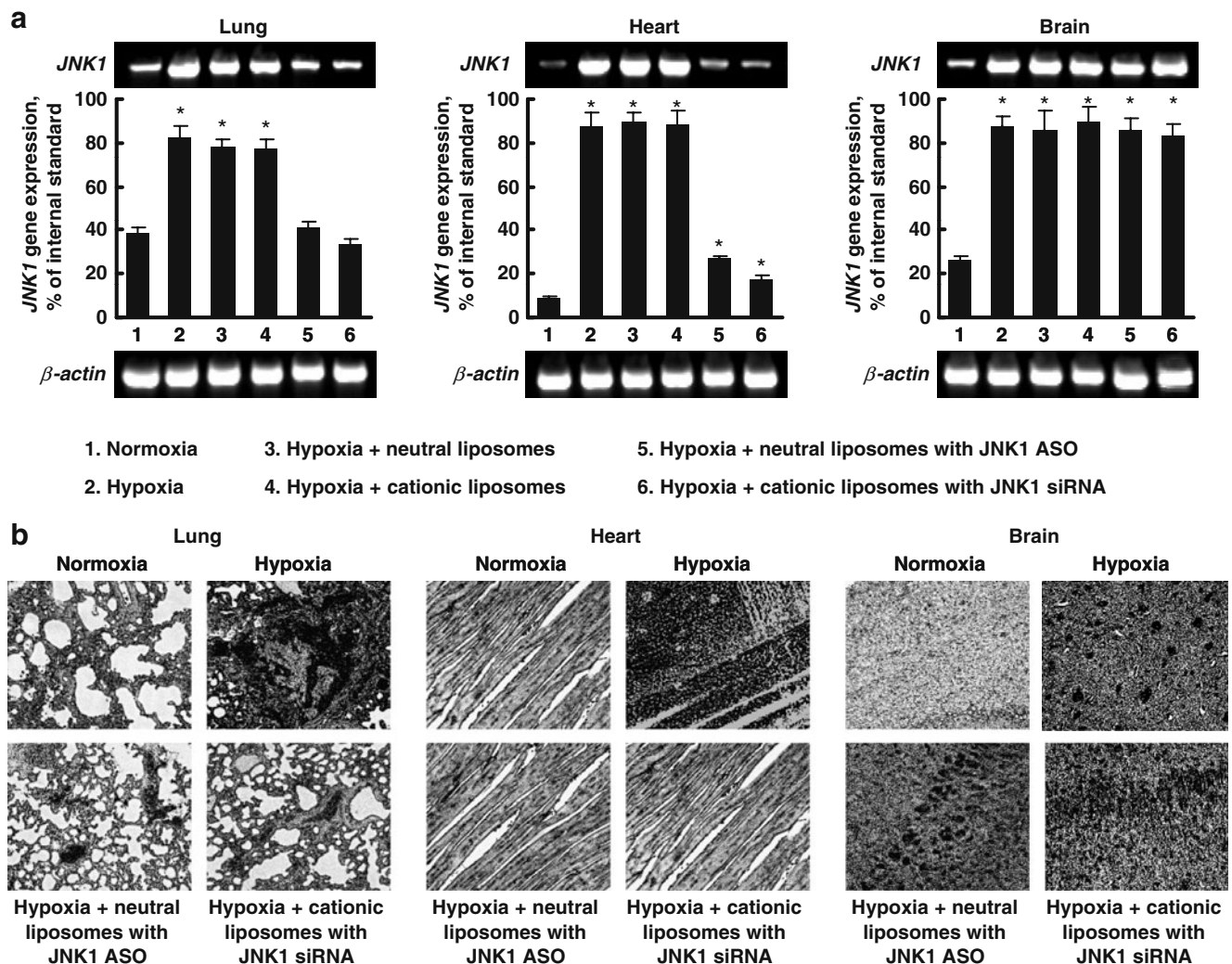


Fig. 5 Expression of JNK1 gene and protein in mouse organs under normoxia and hypoxia. Hypoxia was induced in mice by the inhalation of gas mixture containing 6% O₂ for 2 h. Control mice (normoxia, 1) breathed room air (21% O₂) in the same chamber as animals with hypoxia. Mice were treated with saline (normoxia–control, 1; hypoxia, 2) and indicated substances (3–6) immediately before the

exposure. **a** Typical gel electrophoresis images of RT-PCR products and average expression of the *JNK1* gene. Gene expression was calculated as a ratio of band intensity of *JNK1* gene to that of internal standard (*b-actin*). Means±SD are shown. **P*<0.05 when compared with control. **b** Typical images of tissue sections stained with antibody against JNK1 protein. *Dark color* indicates high protein expression

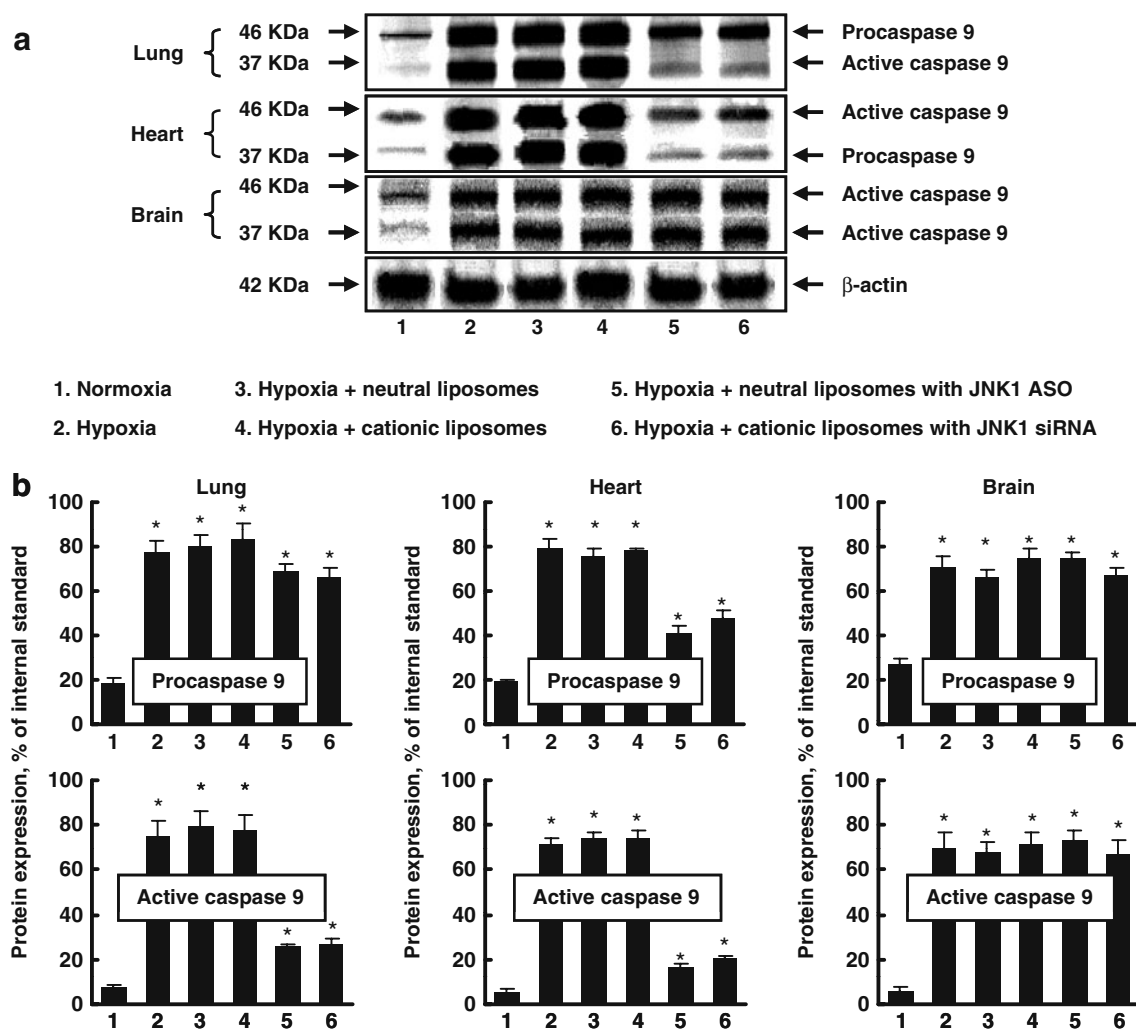


Fig. 6 Expression of caspase 9 in mouse organs under normoxia and hypoxia. Hypoxia was induced in mice by the inhalation of gas mixture containing 6% O₂ for 2 h. Control mice (normoxia, 1) breathed room air (21% O₂) in the same chamber as animals with hypoxia. Mice were treated with saline (normoxia–control, 1; hypoxia, 2) and indicated substances (3–6) immediately before the

exposure. **a** Representative images of Western blots of procaspase and active caspase 9 and β-actin (internal standard) proteins and **b** densitometric analysis of bands. Band intensities of pro- and active caspase 9 are expressed as the percentage of the β-actin band intensity, which was set at 100%. Means±SD are shown. **P*<0.05 when compared with control

studied the expression of the main cell death signaling protein—caspase 9 and apoptosis induction in the selected tissues. The data show that hypoxia led to the overexpression of both procaspase and active caspase 9 (compare Fig. 6a (lanes 1 and 2) and b (bars 1 and 2)) in all studied organs. Empty liposomes (neutral and cationic) did not lead to substantial changes in the expression of procaspase and active caspase 9 (Fig. 6a (lanes 3 and 4), b (bars 3 and 4)). Systemic delivery of ASO and siRNA prior to hypoxia limited the activation of this pathway of apoptosis leading to the decrease in the expression of both procaspase and active caspase 9 in the lungs and heart (Fig. 6a (lanes 5 and 6), b (bars 5 and 6)). In contrast, treatment of mice with liposomal ASO and siRNA did not influence the expression of these proteins in the brain under hypoxia. The direct measure-

ments of apoptosis induction in the tissues showed that hypoxia induced cell death in all studied organs (Fig. 7). In fact, enrichment of histone-associated DNA fragments (mono- and oligo-nucleosomes) in homogenates of the lungs was increased 22–27 times in the lungs and 12–15 times in the heart and brain (compare bars 1 and 2, hypoxia, in Fig. 7). Similar to the expression of pro-apoptotic caspase 9 protein, empty liposomes did not influence significantly on the level of apoptosis in all organs in normoxia and hypoxia (Fig. 7 (bars 2 and 3)). In contrast, ASO or siRNA delivered by liposomes into the cells after their systemic administration significantly limited hypoxic activation of cell death in the lungs and brain (Fig. 7 (bars 4 and 5, hypoxia)).

As an example of tissue histological changes, lung tissues of mice exposed to 6% oxygen for 2 h were used.

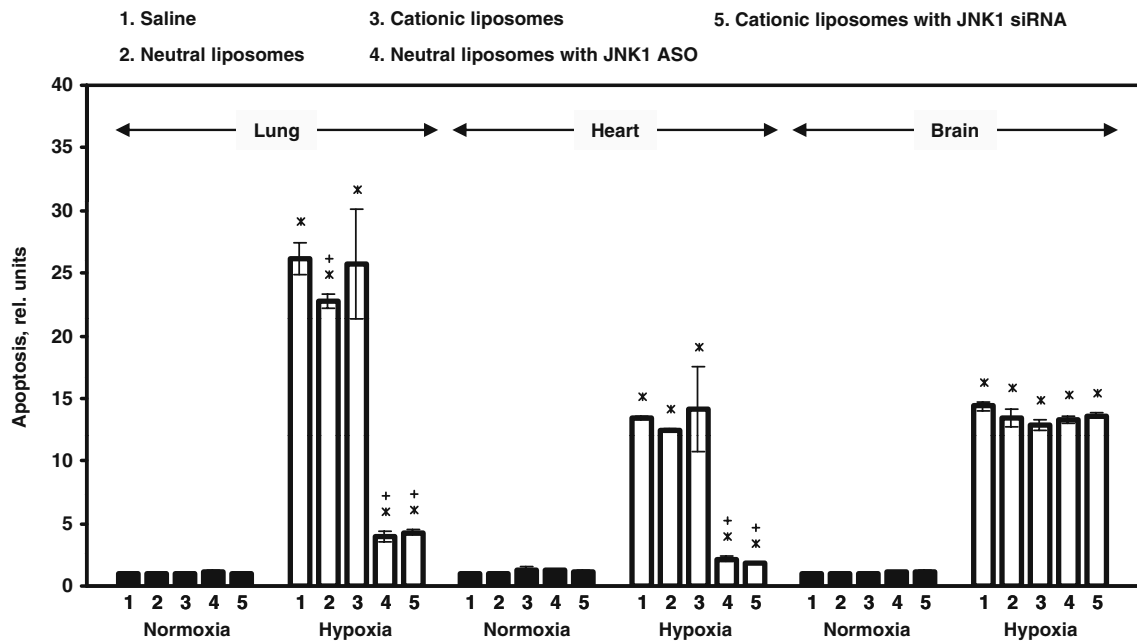


Fig. 7 Apoptosis intensity in different organs of mice during normoxia and hypoxia. Hypoxia was induced in mice by the inhalation of gas mixture containing 6% O₂ for 2 h. Control mice (normoxia) breathed room air (21% O₂) in the same chamber as

animals with hypoxia. Mice were treated with indicated substances immediately before the exposure. Means±SD are shown. **P*<0.05 when compared with normoxia. +*P*<0.05 when compared with hypoxic mice treated with saline

Hematoxylin-eosin stain of lung tissue under normoxia and hypoxia showed that hypoxia led to the serious lung injury. In addition to apoptosis, hypoxia caused necrotic cell death. As shown in the bottom panel of Fig. 8, lung tissue edema

is observed under hypoxia (no treatment). In mice treated with liposomal ASO and siRNA targeted to JNK1 mRNA, necrotic damage and edema produced by hypoxia were significantly less pronounced. In correlation with the organ

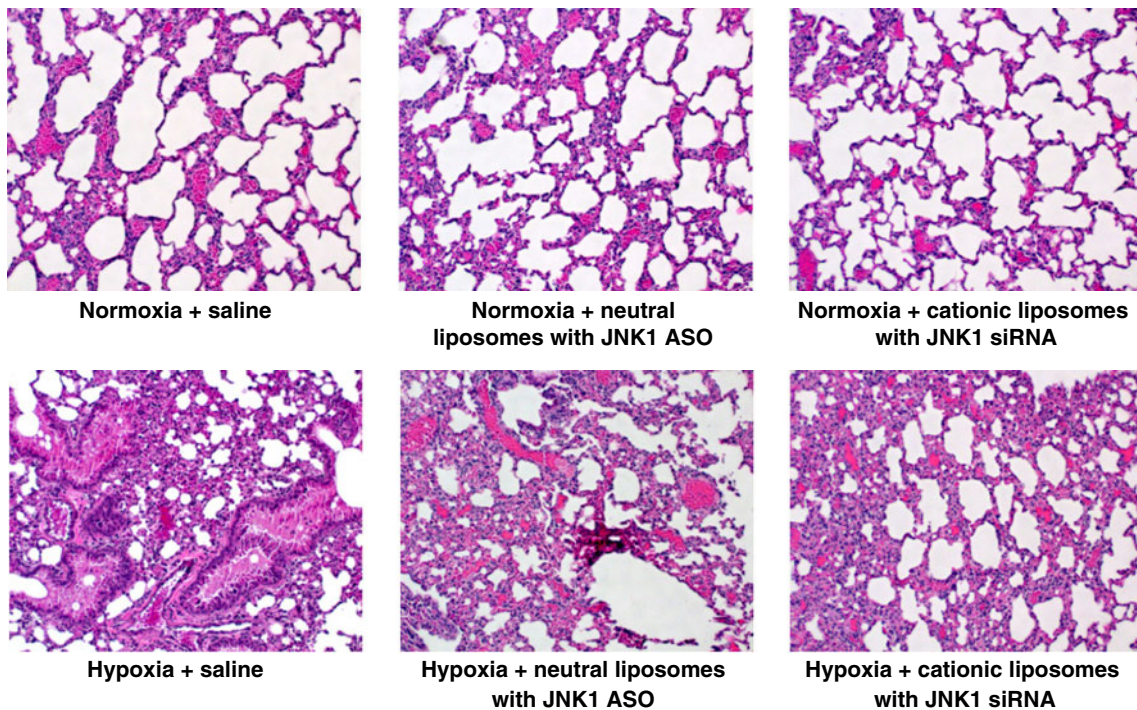


Fig. 8 Typical light microscopy images of lung tissue sections stained with hematoxylin-eosin. Hypoxia was induced in mice by the inhalation of gas mixture containing 6% O₂ for 2 h. Control mice

(normoxia) breathed room air (21% O₂) in the same chamber as animals with hypoxia. Mice were treated with saline and indicated substances immediately before the exposure

distribution of liposomal ASO and siRNA, treatment of mice breathing hypoxic gas mixture with liposomes containing ASO or complexed with siRNA did not influence the hypoxic tissue and cellular damage in the brain (Figs. 4, 5, 6, and 7).

Discussion

Based on the analysis of literature data (Bennett et al. 2001; Zhou et al. 2004) and our previously reported in vitro results (Betigeri et al. 2006), we hypothesized that suppression of JNK1 protein will limit cell death and tissue damage induced by severe hypoxia. To verify our hypothesis, we carried out experiments on mice exposed to exogenous hypoxia caused by inhalation of gas mixture containing 6% oxygen. In order to suppress JNK1 protein, we used neutral liposomes containing P-ethoxy-modified electrically neutral ASO and cationic liposomes complexed with siRNA. ASO and siRNA were designed to suppress JNK protein expression. The liposomes containing active payload were intravenously injected into the tail vein of the mice before hypoxic exposure. Control mice received saline or empty liposomes of both types. As expected, breathing a gas mixture containing 6% O₂ within 2 h induced severe hypoxia associated with lactic acid accumulation in all studied organs. This tissue hypoxia induced caspase-dependent cell death signaling pathway and led to substantial apoptosis induction and tissue damage. After systemic administration, ASO or siRNA delivered by liposomes accumulated in all studied organs excluding the brain. This led to the suppression of targeted JNK1 protein, break down of the cell death signal, limited apoptosis, necrosis and tissue damage under hypoxic exposure. The observed suppression of cell death was evident only in organs with substantial accumulation of liposomal ASO or siRNA, which confirmed that the inhibition of targeted protein following hypoxic cellular damage was caused by ASO or siRNA targeted to JNK1 mRNA delivered by liposomes. Consequently, the defensive action of the treatment was associated with the direct local suppression of targeted JNK1 protein but not with other systemic effects. Therefore, we were able to verify the hypothesis and provide proof of concept of a unique approach to the prevention of cellular damage under severe hypoxia by the suppression of JNK1 hypoxic pathways.

Other approaches can be potentially used separately or in combination with the suppression of JNK1 to limit or prevent tissue damage during hypoxia (Minko et al. 2005). Previously we have shown that antioxidant α -tocopherol delivered by liposomes significantly limited hypoxic damage under lung edema (Minko et al. 2002). Liposomal antioxidant agents were also successfully used to protect organs from ischemic

damage (Rivera et al. 2008; Sinha et al. 2001). In addition, gene delivery into ischemic myocardium by double-targeted lipoplexes with anti-myosin antibody and TAT peptide was tested (Ko et al. 2009). Therefore, the combination of gene and antioxidant therapy has high potential in treatment of hypoxic tissue damage.

The experimental data clearly showed the correlation between the accumulation of delivered ASO or siRNA in organs and anti-hypoxic effect of the treatment. In fact, relatively high accumulation of liposomes and their payload in the lungs and heart substantially limited cell death induction in these organs. In contrast, a trace amount of liposomes, ASO and siRNA accumulated in the brain after systemic administration and was not able to prevent hypoxic brain tissue damage. Therefore, a different strategy and thus a special approach to the delivery through the blood–brain barrier should be used in order to prevent the damage to the brain during severe hypoxia. Conjugation of liposomes with TAT peptide (Gupta et al. 2007; MacKay et al. 2008; Rapoport and Lorberboum-Galski 2009) or transferrin (Soni et al. 2008) potentially can be used in order to accomplish the penetration of liposomes via the blood–brain barrier and delivery of drugs and other active components to the brain.

Acknowledgments This work was supported in part by CA111766 and CA100098 NIH grants.

Open Access This article is distributed under the terms of the Creative Commons Attribution Noncommercial License which permits any noncommercial use, distribution, and reproduction in any medium, provided the original author(s) and source are credited.

References

- Bennett BL, Sasaki DT, Murray BW, O'Leary EC, Sakata ST, Xu W, Leisten JC, Motiwala A, Pierce S, Satoh Y, Bhagwat SS, Manning AM, Anderson DW (2001) SP600125, an anthrapyrazolone inhibitor of Jun N-terminal kinase. *Proc Natl Acad Sci USA* 98:13681–13686
- Betigeri S, Pakunlu RI, Wang Y, Khandare JJ, Minko T (2006) JNK1 as a molecular target to limit cellular mortality under hypoxia. *Mol Pharm* 3:424–430
- Blokhina O, Fagerstedt KV (2010) Oxidative metabolism, ROS and NO under oxygen deprivation. *Plant Physiol Biochem* 48:359–373
- Boning D, Rojas J, Serrato M, Reyes O, Coy L, Mora M (2008) Extracellular pH defense against lactic acid in untrained and trained altitude residents. *Eur J Appl Physiol* 103:127–137
- Busl KM, Greer DM (2010) Hypoxic-ischemic brain injury: pathophysiology, neuropathology and mechanisms. *NeuroRehabilitation* 26:5–13
- Carlsson Y, Leverin AL, Hedtjam M, Wang X, Mallard C, Hagberg H (2009) Role of mixed lineage kinase inhibition in neonatal hypoxia-ischemia. *Dev Neurosci* 31:420–426
- Chihab R, Ferry C, Koziel V, Monin P, Daval JL (1998) Sequential activation of activator protein-1-related transcription factors and JNK protein kinases may contribute to apoptotic death induced

- by transient hypoxia in developing brain neurons. *Brain Res Mol Brain Res* 63:105–120
- Cho DH, Lee HJ, Kim HJ, Hong SH, Pyo JO, Cho C, Jung YK (2007a) Suppression of hypoxic cell death by AIP-induced sustained activation of AKT and ERK1/2. *Oncogene* 26:2809–2814
- Cho YE, Ko JH, Kim YJ, Yim JH, Kim SM, Park JH (2007b) mHGT-D-P mediates hypoxic neuronal cell death via the release of apoptosis-inducing factor. *Neurosci Lett* 416:144–149
- Corbucci GG, Marchi A, Lettieri B, Luongo C (2005) Mechanisms of cell protection by adaptation to chronic and acute hypoxia: molecular biology and clinical practice. *Minerva Anestesiol* 71:727–740
- Crenesse D, Laurens M, Heurteaux C, Cursio R, Saint-Paul MC, Schmid-Alliana A, Gugenheim J (2003) Rat liver ischemia-reperfusion-induced apoptosis and necrosis are decreased by FK506 pretreatment. *Eur J Pharmacol* 473:177–184
- Danielyan L, Buniatian GH, Gleiter CH (2006) Common neuroprotective effects of endothelin receptor blockade and erythropoietin during hypoxia-associated cell injury. Perspectives of combined treatment. *Scientific World Journal* 6:449–451
- Derijard B, Hibi M, Wu IH, Barrett T, Su B, Deng T, Karin M, Davis RJ (1994) JNK1: a protein kinase stimulated by UV light and Ha-Ras that binds and phosphorylates the c-Jun activation domain. *Cell* 76:1025–1037
- Dhar-Mascareno M, Carcamo JM, Golde DW (2005) Hypoxia-reoxygenation-induced mitochondrial damage and apoptosis in human endothelial cells are inhibited by vitamin C. *Free Radic Biol Med* 38:1311–1322
- Dharap SS, Wang Y, Chandna P, Khandare JJ, Qiu B, Gunaseelan S, Sinko PJ, Stein S, Farmanfarmaian A, Minko T (2005) Tumor-specific targeting of an anticancer drug delivery system by LHRH peptide. *Proc Natl Acad Sci USA* 102:12962–12967
- Freiberg RA, Krieg AJ, Giaccia AJ, Hammond EM (2006) Checking in on hypoxia/reoxygenation. *Cell Cycle* 5:1304–1307
- Garay M, Gaarde W, Monia BP, Nero P, Cioffi CL (2000) Inhibition of hypoxia/reoxygenation-induced apoptosis by an antisense oligonucleotide targeted to JNK1 in human kidney cells. *Biochem Pharmacol* 59:1033–1043
- Garbuzenko OB, Saad M, Betigeri S, Zhang M, Vetcher AA, Soldatenkov VA, Reimer DC, Pozharov VP, Minko T (2009) Intratracheal versus intravenous liposomal delivery of siRNA, antisense oligonucleotides and anticancer drug. *Pharm Res* 26:382–394
- Garbuzenko OB, Saad M, Pozharov VP, Reuhl KR, Mainelis G, Minko T (2010) Inhibition of lung tumor growth by complex pulmonary delivery of drugs with oligonucleotides as suppressors of cellular resistance. *Proc Natl Acad Sci USA* 107:10737–10742
- Gonchar O, Mankovskaya I (2009) Effect of moderate hypoxia/reoxygenation on mitochondrial adaptation to acute severe hypoxia. *Acta Biol Hung* 60:185–194
- Goni-de-Cerio F, Alvarez A, Caballero A, Mielgo VE, Alvarez FJ, Rey-Santano MC, Gastiasoro E, Valls-i-Soler A, Bilbao J, Hilario E (2007) Early cell death in the brain of fetal preterm lambs after hypoxic-ischemic injury. *Brain Res* 1151:161–171
- Gupta B, Levchenko TS, Torchilin VP (2007) TAT peptide-modified liposomes provide enhanced gene delivery to intracranial human brain tumor xenografts in nude mice. *Oncol Res* 16:351–359
- Hellwig-Burgel T, Stiehl DP, Wagner AE, Metzen E, Jelkmann W (2005) Review: hypoxia-inducible factor-1 (HIF-1): a novel transcription factor in immune reactions. *J Interferon Cytokine Res* 25:297–310
- Hossain MA (2008) Hypoxic-ischemic injury in neonatal brain: involvement of a novel neuronal molecule in neuronal cell death and potential target for neuroprotection. *Int J Dev Neurosci* 26:93–101
- Hreniuk D, Garay M, Gaarde W, Monia BP, McKay RA, Cioffi CL (2001) Inhibition of c-Jun N-terminal kinase 1, but not c-Jun N-terminal kinase 2, suppresses apoptosis induced by ischemia/reoxygenation in rat cardiac myocytes. *Mol Pharmacol* 59:867–874
- Hung TH, Burton GJ (2006) Hypoxia and reoxygenation: a possible mechanism for placental oxidative stress in preeclampsia. *Taiwan J Obstet Gynecol* 45:189–200
- Karin M (1995) The regulation of AP-1 activity by mitogen-activated protein kinases. *J Biol Chem* 270:16483–16486
- Kim BM, Choi JY, Kim YJ, Woo HD, Chung HW (2007) Reoxygenation following hypoxia activates DNA-damage checkpoint signaling pathways that suppress cell-cycle progression in cultured human lymphocytes. *FEBS Lett* 581:3005–3012
- Kim JY, Ahn HJ, Ryu JH, Suk K, Park JH (2004) BH3-only protein Noxa is a mediator of hypoxic cell death induced by hypoxia-inducible factor 1alpha. *J Exp Med* 199:113–124
- Kim JY, Park JH (2003) ROS-dependent caspase-9 activation in hypoxic cell death. *FEBS Lett* 549:94–98
- Ko YT, Hartner WC, Kale A, Torchilin VP (2009) Gene delivery into ischemic myocardium by double-targeted lipoplexes with anti-myosin antibody and TAT peptide. *Gene Ther* 16:52–59
- Kothari S, Cizeau J, McMillan-Ward E, Israels SJ, Bailes M, Ens K, Kirshenbaum LA, Gibson SB (2003) BNP3 plays a role in hypoxic cell death in human epithelial cells that is inhibited by growth factors EGF and IGF. *Oncogene* 22:4734–4744
- Lecour S, Van der Merwe E, Opie LH, Sack MN (2006) Ceramide attenuates hypoxic cell death via reactive oxygen species signaling. *J Cardiovasc Pharmacol* 47:158–163
- MacKay JA, Li W, Huang Z, Dy EE, Huynh G, Tihan T, Collins R, Deen DF, Szoka FC Jr (2008) HIV TAT peptide modifies the distribution of DNA nanolipoparticles following convection-enhanced delivery. *Mol Ther* 16:893–900
- Meerson F, Pozharov V, Minyailenko T (1994) Superresistance against hypoxia after preliminary adaptation to repeated stress. *J Appl Physiol* 76:1856–1861
- Millet GP, Roels B, Schmitt L, Woorons X, Richalet JP (2010) Combining hypoxic methods for peak performance. *Sports Med* 40:1–25
- Minciu Macrea M, Misra H, Zagrean L (2010) The neuroprotective effect of intranasally applied leptin against hypoxic neuronal injury. *Med Hypotheses* 74:1036–1037
- Minko T, Kopeckova P, Kopecek J (1999) Comparison of the anticancer effect of free and HPMA copolymer-bound adriamycin in human ovarian carcinoma cells. *Pharm Res* 16:986–996
- Minko T, Stefanov A, Pozharov V (2002) Selected contribution: lung hypoxia: antioxidant and antiapoptotic effects of liposomal alfacetopheryl. *J Appl Physiol* 93:1550–1560, discussion 1549
- Minko T, Wang Y, Pozharov V (2005) Remediation of cellular hypoxic damage by pharmacological agents. *Curr Pharm Des* 11:3185–3199
- Murray J, Walmsley SR, Mecklenburgh KI, Cowburn AS, White JF, Rossi AG, Chilvers ER (2003) Hypoxic regulation of neutrophil apoptosis role: of reactive oxygen intermediates in constitutive and tumor necrosis factor alpha-induced cell death. *Ann NY Acad Sci* 1010:417–425
- Myllyharju J (2008) Prolyl 4-hydroxylases, key enzymes in the synthesis of collagens and regulation of the response to hypoxia, and their roles as treatment targets. *Ann Med* 40:402–417
- Nagel S, Talbot NP, Mecnovic J, Smith TG, Buchan AM, Schofield CJ (2010) Therapeutic manipulation of the HIF hydroxylases. *Antioxid Redox Signal* 12:481–501
- Ostadal B, Kolar F (2007) Cardiac adaptation to chronic high-altitude hypoxia: beneficial and adverse effects. *Respir Physiol Neurobiol* 158:224–236
- Pakunlu RI, Cook TJ, Minko T (2003) Simultaneous modulation of multidrug resistance and antiapoptotic cellular defense by MDR1 and BCL-2 targeted antisense oligonucleotides enhances the anticancer efficacy of doxorubicin. *Pharm Res* 20:351–359
- Pakunlu RI, Wang Y, Saad M, Khandare JJ, Starovoytov V, Minko T (2006) In vitro and in vivo intracellular liposomal delivery of

- antisense oligonucleotides and anticancer drug. *J Control Release* 114:153–162
- Pakunlu RI, Wang Y, Tsao W, Pozharov V, Cook TJ, Minko T (2004) Enhancement of the efficacy of chemotherapy for lung cancer by simultaneous suppression of multidrug resistance and antiapoptotic cellular defense: novel multicomponent delivery system. *Cancer Res* 64:6214–6224
- Patil ML, Zhang M, Betigeri S, Taratula O, He H, Minko T (2008) Surface-modified and internally cationic polyamidoamine dendrimers for efficient siRNA delivery. *Bioconjug Chem* 19:1396–1403
- Portugal-Cohen M, Kohen R (2009) Exposure of human keratinocytes to ischemia, hyperglycemia and their combination induces oxidative stress via the enzymes inducible nitric oxide synthase and xanthine oxidase. *J Dermatol Sci* 55:82–90
- Rapoport M, Lorberboum-Galski H (2009) TAT-based drug delivery system—new directions in protein delivery for new hopes? *Expert Opin Drug Deliv* 6:453–463
- Ricci L, Valoti M, Sgaragli G, Frosini M (2009) Protection by taurine of rat brain cortical slices against oxygen glucose deprivation- and reoxygenation-induced damage. *Eur J Pharmacol* 621:26–32
- Rivera F, Costa G, Abin A, Urbanavicius J, Arruti C, Casanova G, Dajas F (2008) Reduction of ischemic brain damage and increase of glutathione by a liposomal preparation of quercetin in permanent focal ischemia in rats. *Neurotox Res* 13:105–114
- Sinha J, Das N, Basu MK (2001) Liposomal antioxidants in combating ischemia-reperfusion injury in rat brain. *Biomed Pharmacother* 55:264–271
- Soleymanlou N, Jurisicova A, Wu Y, Chijiwa M, Ray JE, Detmar J, Todros T, Zamudio S, Post M, Caniggia I (2007) Hypoxic switch in mitochondrial myeloid cell leukemia factor-1/Mtd apoptotic rheostat contributes to human trophoblast cell death in pre-eclampsia. *Am J Pathol* 171:496–506
- Soni V, Kohli DV, Jain SK (2008) Transferrin-conjugated liposomal system for improved delivery of 5-fluorouracil to brain. *J Drug Target* 16:73–78
- Surova OV, Nagibin VS, Tumanovskaya LV, Dosenko VE, Moibenko AA (2009) Effect of a low dose of proteasome inhibitor on cell death and gene expression in neonatal rat cardiomyocyte cultures exposed to anoxia-reoxygenation. *Exp Clin Cardiol* 14:e57–e61
- Vacotto M, Coso O, Fiszer de Plazas S (2008) Programmed cell death and differential JNK, p38 and ERK response in a prenatal acute hypoxic hypoxia model. *Neurochem Int* 52:857–863
- Wang Y, Minko T (2004) A novel cancer therapy: combined liposomal hypoxia inducible factor 1 alpha antisense oligonucleotides and an anticancer drug. *Biochem Pharmacol* 68:2031–2042
- Wang Y, Pakunlu RI, Tsao W, Pozharov V, Minko T (2004) Bimodal effect of hypoxia in cancer: the role of hypoxia inducible factor in apoptosis. *Mol Pharm* 1:156–165
- Wang Y, Saad M, Pakunlu RI, Khandare JJ, Garbuzenko OB, Vetcher AA, Soldatenkov VA, Pozharov VP, Minko T (2008) Nonviral nanoscale-based delivery of antisense oligonucleotides targeted to hypoxia-inducible factor 1{alpha} enhances the efficacy of chemotherapy in drug-resistant tumor. *Clin Cancer Res* 14:3607–3616
- Wenger RH, Camenisch G, Stiehl DP, Katschinski DM (2009) HIF prolyl-4-hydroxylase interacting proteins: consequences for drug targeting. *Curr Pharm Des* 15:3886–3894
- Yajima D, Motani H, Hayakawa M, Sato Y, Sato K, Iwase H (2009) The relationship between cell membrane damage and lipid peroxidation under the condition of hypoxia-reoxygenation: analysis of the mechanism using antioxidants and electron transport inhibitors. *Cell Biochem Funct* 27:338–343
- Zhao Y, Chen XQ, Du JZ (2009) Cellular adaptation to hypoxia and p53 transcription regulation. *J Zhejiang Univ Sci B* 10:404–410
- Zhou G, Golden T, Aragon IV, Honkanen RE (2004) Ser/Thr protein phosphatase 5 inactivates hypoxia-induced activation of an apoptosis signal-regulating kinase 1/MKK-4/JNK signaling cascade. *J Biol Chem* 279:46595–46605
- Zhu H, Wang WJ, Ding WL, Li F, He J (2008) Effect of panaxydol on hypoxia-induced cell death and expression and secretion of neurotrophic factors (NTFs) in hypoxic primary cultured Schwann cells. *Chem Biol Interact* 174:44–50